RSC Advances

PAPER

View Article Online
View Journal | View Issue

Cite this: *RSC Adv.*, 2017, **7**, 21268

A new *mfj*-type metal–organic framework constructed from a methoxyl derived V-shaped ligand and its H_2, CO_2 and CH_4 adsorption properties†

Liting Du,[ac] Zhiyong Lu,[*b] Li Xu[c] and Jinchi Zhang[*a]

Received 20th February 2017
Accepted 10th April 2017

DOI: 10.1039/c7ra02122d

rsc.li/rsc-advances

Based on a new V-shaped tetracarboxylic ligand with a methoxyl group, a new *mfj*-type microporous metal–organic framework $[Cu_6(MBDPB)_3(H_2O)_6]\cdot 12DMF\cdot 10H_2O$ (NJFU-3, NJFU for Nanjing Forestry University; H_4MBDPB for 5-methoxyl-1,3-bis(3,5-dicarboxylphenyl)-benzene) was successfully synthesized and structurally characterized. With moderately high porosity, appropriate pore aperture and unsaturated metal sites, the activated NJFU-3a exhibits high H_2 (2.56 wt% at 77 K and 1 bar) and CO_2 uptakes (15.8 wt% at 298 K and 1 bar), and a moderately high CH_4 storage capacity of 155 cm^3 cm^{-3} at 35 bar and 298 K. Meanwhile, it shows a comparably high delivery amount of 135 cm^3 cm^{-3} when taking 5 bar as a specific lower pressure limit and 65 bar as the upper limit.

Introduction

Metal–organic frameworks (MOFs) or porous coordination polymers have emerged as a new type of porous materials with regular arrays of metal ions, or metal clusters and organic linkers.[1–6] Because the pore sizes can be finely tuned and the functional sites can be deliberately immobilized on the pore surfaces, MOFs have unique properties and wide applications in gas storage, molecule separation, chemical sensing, catalysis, and drug delivery. Among them, gas storage concerning H_2, CO_2 and CH_4 is the most investigated in recent years.[7–16]

Due to their intriguing structures and excellent gas adsorption properties, MOFs constructed from tetracarboxylic ligands have attracted great attention and are widely investigated by many research groups.[17–27] NbO-type MOFs, built from linear tetracarboxylic ligands and dicopper paddlewheel clusters, show their advantages in hydrogen adsorption as well as methane storage.[10,24] The NOTT-MOFs synthesized by the Schröder group not only exhibit high H_2 uptake capacities, but were further proved to be excellent candidates for methane storage. Therefore, based on this type of structure, deeper and thorough tuning towards better performance in gas storage has been reported thereafter. Besides NbO-MOFs, building other types of MOFs from non-linear tetracarboxylic ligands, V-shaped ligands for instance, is another field of endeavour.[28–33] These non-NbO-type MOFs also demonstrated their great potential in hydrogen adsorption and methane storage, as illustrated by PCN-12 (ref. 28) and PCN-14.[23] However, the dynamic nature of ligands endows these MOFs great structural variability, which causes difficulties in property optimization. Therefore, a stable structural platform for isoreticular optimization is of great importance. PCN-306, as a rare MOF with (3,3,4,4)-connected *mfj*-type network, represents a suitable structural prototype for further tailoring among MOFs constructed by V-shaped tetracarboxylic ligands.[34] Our previous work on NJU-Bai10, an analogue of PCN-306, exhibits high hydrogen uptake and high methane storage property.[35]

In order to achieve high performance of gas adsorption in MOFs, isorecticular optimization based on a stable structural platform by ligand functionalization is widely applied. Among them, polar functional groups are most preferred.[36] Methoxy group, as a common polar functional group, has been proved effective in some cases in the adsorption of gases like CO_2 and hydrocarbon.[37–39] Inspired by these works, herein we designed and incorporated the bulky methoxy groups (Scheme 1) into the framework of PCN-306 to form an another *mfj*-type MOF $[Cu_6(MBDPB)_3(H_2O)_6]\cdot 12DMF\cdot 10H_2O$ (NJFU-3, NJFU for Nanjing Forestry University; H_4MBDPB for 5-methoxyl-1,3-bis(3,5-dicarboxylphenyl)-benzene). Interestingly, the incorporation of methoxy groups was able to improve the gas adsorption property of NJFU-3 not by its polarity, but through optimizing the inner textural property of NJFU-3. As a result, the activated

[a]*Collaborative Innovation Center of Sustainable Forestry in Southern China of Jiangsu Province, Nanjing Forestry University, Nanjing, 210037, China. E-mail: zhang8811@njfu.edu.cn*

[b]*College of Mechanics and Materials, Hohai University, Nanjing 210098, China. E-mail: johnlook1987@gmail.com*

[c]*Advanced Analysis and Testing Center, Nanjing Forestry University, Nanjing 210037, China*

† Electronic supplementary information (ESI) available: Experimental details, PXRD patterns, heat of adsorption. CCDC 1532967. For ESI and crystallographic data in CIF or other electronic format see DOI: 10.1039/c7ra02122d

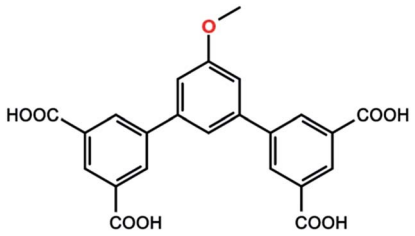

Scheme 1 The ligand of H_4MBDPB.

NJFU-3a exhibits a high hydrogen adsorption of 2.56 wt% at 77 K and 1 bar and a high CO_2 uptake of 15.8 wt% at 298 K and 1 bar. Meanwhile, it shows a moderately high CH_4 storage of 155 cm^3 cm^{-3} at 35 bar and 298 K and a quite large CH_4 delivery amount of 135 cm^3 cm^{-3}, which indicates it as a potential material for CH_4 storage.

Experimental

Materials and methods

All chemical reagents were obtained from commercial sources and, unless otherwise noted, were used as received without further purification. Elemental analyses (C, H, and N) were performed on a Perkin-Elmer 240 analyzer. The IR spectra were recorded in the 400–4000 cm^{-1} on a Bruker VERTEX 80V spectrometer using KBr pellets. ^{1}H NMR spectra were recorded on a Bruker DRX-500 spectrometer with tetramethylsilane as an internal reference. Thermal gravimetric analyses (TGA) were performed under N_2 atmosphere (100 mL min^{-1}) with a heating rate of 5 °C min^{-1} using a 2960 SDT thermogravimetric analyzer. Powder X-ray diffraction (PXRD) data were collected on a Bruker D8 ADVANCE X-ray diffractometer with Cu/Kα radiation.

Gas sorption measurements

Low pressure gas sorption measurements were conducted using a Micromeritics ASAP 2020 surface area and pore size analyzer up to saturated pressure at different temperatures. High pressure gravimetric CH_4 adsorption measurements were performed on an ISOSORP HyGpra + V adsorption analyzer (Rubotherm, Germany) over 0–65 bar range at 298 K. Before the gas sorption measurement, more than 150 mg (about 100 mg for high pressure gas adsorption) as-synthesized samples of NJFU-3 were washed with DMF and methanol, respectively. Fresh anhydrous methanol was then added, and the samples were allowed to soak for 3 days for solvent-exchange. During this period, methanol was refreshed every 8 hours. After then, the sample was charged into a sample tube and activated at 90 °C for 20 hours under vacuum.

X-ray collection and structure determination

Single crystal suitable for X-ray structure determination were selected and sealed in a capillary under a microscope. The X-ray diffraction intensity data were measured on a BRUKER D8 VENTURE PHOTON diffractometer at room temperature using graphite monochromated Mo/Kα radiation (λ = 0.71073 Å). Data reduction was made with the Bruker Saint program. The structures were solved by direct methods and refined with full-matrix least squares technique using the SHELXTL package. Non-hydrogen atoms were refined with anisotropic displacement parameters during the final cycles. Hydrogen atoms were placed in calculated positions with isotropic displacement parameters set to 1.2 × U_{eq} of the attached atom. The unit cell includes a large region of disordered solvent molecules, which could not be modeled as discrete atomic sites. We employed PLATON/SQUEEZE to calculate the diffraction contribution of the solvent molecules and, thereby, to produce a set of solvent-free diffraction intensities; structures were then refined again using the data generated. Crystal data and refinement conditions are shown in Table S1.† The crystal data for NJFU-3‡ have been deposited in CSD database, and labeled as 1532967.

Synthesis and characterization

The organic linker 5-methoxyl-1,3-bis(3,5-dicarboxylphenyl)-benzene (H_4MBDPB) (Scheme 1) was readily synthesized according to ref. 6. ^{1}H NMR (500 MHz, DMSO-*d*6): 13.31 (bs, 4H), 8.40 (s, 2H), 8.36 (s, 4H), 7.49 (s, 1H), 7.22 (s, 2H), 3.86 (s, 3H). Selected FTIR (neat, cm^{-1}): 3442, 3187, 3085, 2625, 2533, 1701, 1592, 1439, 1389, 1349, 1210, 1139, 1095, 1051, 917, 853, 756, 675. A mixture of H_4MBDPB (5.23 mg, 0.012 mmol) and $CuCl_2 \cdot 2H_2O$ (13.6 mg, 0.08 mmol) was dissolved in DMF/H_2O (2 mL, 5 : 1, v/v) in a screw-capped vial. A concentrated HNO_3 (0.05 mL) (65%, aq.) was added to the mixture, the vial was capped and placed in an oven at 65 °C for 2 days. The resulting blue pyramid-shaped crystals were filtered and washed with DMF several times to give NJFU-3 materials. Yield: 72%. Elemental analysis: calcd for activated Cu_2(MBDPB), %: C, 49.34; H, 2.15; N, 0; found: C, 49.16; H, 2.07; N, 0.02. Selected FTIR (neat, cm^{-1}): 3443, 3071, 2932, 2866, 1671, 1635, 1587, 1498, 1436, 1410, 1368, 1304, 1255, 1216, 1154, 1093, 1052, 935, 864, 807, 776, 731, 661.

Results and discussion

The structure of NJFU-3 was characterized by single-crystal X-ray diffraction measurement, and the phase purity of the bulk material was independently confirmed by powder X-ray diffraction (PXRD). The similarity of the simulated PXRD pattern from single-crystal data to those for both as-synthesized and activated samples reveals that the single crystal is representative of the pure bulk sample, and the framework is robust and its crystallinity can be retained after the removal of guest molecules and the coordinated water molecules (Fig. S1, ESI†). Single-crystal structure determination reveals that NJFU-3 crystallizes in orthorhombic space group *Cmc*2_1, and the symmetric unit consists of one and a half MBDPB-ligand, three crystallographically Cu^{2+} ions and three coordinated water molecule (Fig. S2†). Two types of MBDPB-ligands existed in the structure possess

‡ Crystal data for NJFU-3: $C_{69}H_{36}Cu_6O_{33}$, M = 1774.28, orthorhombic, *Cmc*2_1, a = 24.742(3) Å, b = 33.475(3) Å, c = 18.4621(19) Å, $\alpha = \beta = \gamma = 90°$, V = 15 291 (3) $Å^3$, Z = 4, D_c = 0.771 g cm^{-3}, GOF = 0.984 based on F^2, final R_1 = 0.0729, wR_2 = 0.1842 [for 18 616 data $I > 2\sigma(I)$]; data for structure was treated with squeeze.

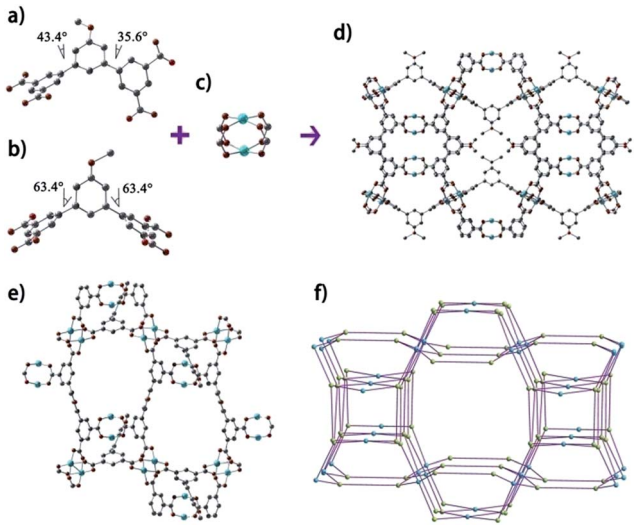

Fig. 1 (a)–(d) are the assembly of two different configurations of ligands and dicopper paddlewheel-clusters into three-dimensional structure; (e) the structure of NJFU-3 viewed along *a* direction; (f) *mfj*-type network simplified from NJFU-3.

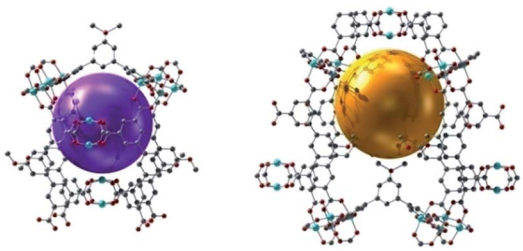

Fig. 2 Two types of cages in NJFU-3: Cage A (purple) and Cage B (orange).

different dihedral angles between central and terminal benzene rings, one (Fig. 1a) with about 43.4° and 35.6° and the other (Fig. 1b) approximately 63.4° and 63.4°. Each MBDPB-ligand links with four 4-connected dicopper paddlewheel SBUs. By simplifying MBDPB-ligands as two 3-connected nodes and regarding the dicopper paddlewheels SBUs as 4-connected nodes, the whole structure adopts a (3,3,4,4)-c 4-nodal *mfj*-topology (Fig. 1c). Just as its isoreticular analogues, there are two types of cages existed in the structure: one is surrounded by seven dicopper SBUs and five MBDPB-ligands (Cage A, Fig. 2a), and the other is assembly by eleven dicopper SBUs and eleven MBDPB-ligands (Cage B, Fig. 2b). The cavity inside Cage A and Cage B is with diameters of about 11 Å (excluding van der Waals radii) and 12 Å, respectively. The inner cavity of NJFU-3 endows it high porosity, as calculated using PLATON routine, with the solvent accessible volume of 74.1% in the dehydrated structure of NJFU-3.

Its permanent porosity as well as gas adsorption properties was further investigated. The phase purity of the bulk sample was confirmed by powder X-ray diffraction (PXRD) (Fig. S1, ESI†) and a weight loss of about 41% at 30–300 °C was observed from the TG curve of NJFU-3, which corresponds to 12 DMF and $16 \cdot H_2O$ molecules (calcd 41.1%) (Fig. S11, ESI†). The methanol solvent-exchanged sample was degassed under high vacuum at 90 °C for 20 hours to obtain the fully activated sample NJFU-3a. A color change from pale-blue to deep-purple-blue occurred, indicating the exposure of unsaturated metal sites in NJFU-3a. The type-I isotherm of N_2 adsorption at 77 K indicates that NJFU-3a is a microporous material. Based on the N_2 adsorption isotherm, the Brunauer–Emmett–Teller (BET) surface area and Langmuir surface area of NJFU-3a are calculated to be 2531.1 m^2 g^{-1} and 2671.9 m^2 g^{-1}, respectively. The total pore volume obtained from N_2 isotherm is 0.94 cm^3 g^{-1}.

The moderately high surface area, large pore volume and unsaturated metal sites within the structure of NJFU-3a encouraged us to study its gas adsorption capacity. Low-pressure hydrogen adsorption measurements of NJFU-3a were performed at 77 K and 87 K. The adsorption isotherms are fully reversible (Fig. S5†), and 2.56 wt% of H_2 uptake for NJFU-3a was observed under the condition of 77 K and 1 bar, which is a bit higher than that of PCN-306 (ref. 34) (2.50 wt%) (Fig. 3b). Meanwhile, the H_2 uptake of NJFU-3a is also higher than that of most of the NOTT-series MOFs constructed by linear tetracarboxylic ligands, such as NOTT-101 (ref. 22) (2.46 wt%), NOTT-109 (ref. 22) (2.28 wt%), NOTT-106 (ref. 22) (2.24 wt%), making it one of the MOFs with highest H_2 uptake capacity at 77 K and 1 bar. The CO_2 adsorption property of NJFU-3a was also measured at 273 K and 298 K. As shown in Fig. 3c, at 298 K and 1 bar, NJFU-3a can absorb 95.6 cm^3 g^{-1} (or 15.8 wt%) of CO_2, which is the highest among all the *mfj*-MOFs such as PCN-306 (ref. 34) (13.8 wt%) and PCN-308 (ref. 34) (15.4 wt%), and is also higher than some well-known MOFs with open metal sites and/or Lewis basic sites, such as en-CuBTTri[40] (5.5 wt%), MOF-505 (ref. 41) (14.4 wt%), Bio-MOF-1 (ref. 42) (14.3 wt%), SNU-21S[43] (11.1 wt%), PCN-61 (ref. 14 and 44) (13.9 wt%), PCN-68 (ref. 14 and 44) (4.84 wt%), MIL-102 (ref. 45) (13.6 wt%), MAF-X7 (ref. 46) (5.13 wt%) and NU-100 (ref. 47) (12 wt%). To

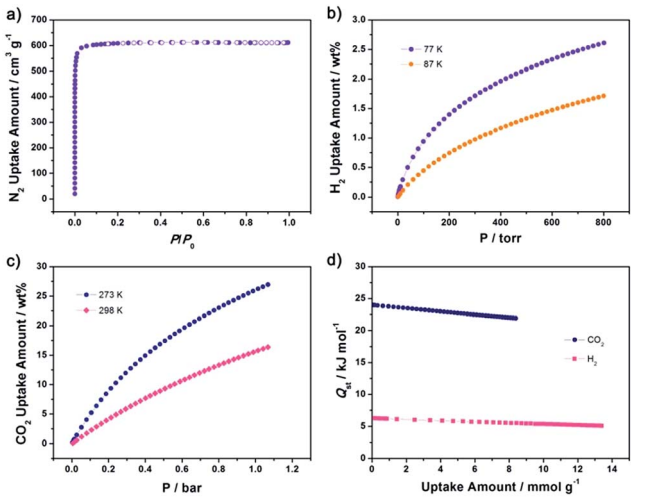

Fig. 3 (a) N_2 adsorption isotherm of NJFU-3a at 77 K; (b) H_2 adsorption isotherms of NJFU-3a at 77 K and 87 K; (c) CO_2 adsorption isotherms of NJFU-3a at 273 K and 298 K; (d) CO_2 and H_2 adsorption enthalpies of NJFU-3a.

further understand the interaction between gases molecules and the framework, we calculated the H_2 and CO_2 adsorption enthalpies of NJFU-3a by virial method, and the zero-coverage values are 6.27 kJ mol^{-1} and 24.0 kJ mol^{-1} for H_2 and CO_2 respectively. Compared with those of the PCN-306, the analogue without methoxyl group, no obvious change was found (H_2: 6.37 kJ mol^{-1}; CO_2: 23.997 kJ mol^{-1}). Therefore, the existence of methoxyl groups in NJFU-3a does not contribute to the enhancement of interactions between gas molecules and framework, but optimizes the inner textural property that leads to the improvement of gas adsorption property at 1 bar. Furthermore, the CH_4 adsorption isotherm of NJFU-3a at 273 K (Fig. S9, ESI†) was also measured to investigate the influence of methoxy group on CO_2/CH_4 selectivity. By applying the Ideal Adsorbed Solution Theory (IAST), the CO_2/CH_4 selectivity of NJFU-3a was predicted to be 7.9 (Fig. S9†), which is a bit higher than that of PCN-306 (7.52). Although not significant, such improvement still indicates the positive effect of methoxy groups on the selective adsorption of CO_2 in this type of MOF.

We further measured the CH_4 storage capacity of NJFU-3a at 298 K. As shown in Fig. 4b, NJFU-3a shows moderately high volumetric methane uptakes of 155 cm^3 cm^{-3} under 35 bar and 298 K, reaching approximately 86% of the DOE standard (180 cm^3 cm^{-3}) at 35 bar and room temperature. The methane storage capacity of NJFU-3a is lower than some of the MOFs with extraordinary high methane storage, but higher than most MOF materials under similar condition (MOF-5,[8] 150 cm^3 cm^{-3}; PCN-80,[48] 118 cm^3 cm^{-3}; ZJU-36,[49] 142 cm^3 cm^{-3}; NU-111,[7] 138 cm^3 cm^{-3}; PCN-66,[44] 136 cm^3 cm^{-3}; UiO-66 (Zr),[50] 146 cm^3 cm^{-3}; MOF-205,[1] 119 cm^3 cm^{-3}). When the pressure reaches 65 bar, the methane storage capacity of NJFU-3a increases up to 189 cm^3 cm^{-3}. Taking 5 bar as a specific lower pressure limit and 65 bar as the upper limit, the methane delivery amounts of NJFU-3a is 135 cm^3 cm^{-3}, that is, a tank filled with NJFU-3a can deliver 51.3% as much fuel as the CNG tank operating at the same lower pressure limit and at 250 bar as the upper limit. Although this value is lower compared to the best performing MOFs, it is still quite comparable with MgMOF-74 (ref. 8) (142 cm^3 cm^{-3}), NiMOF-74 (ref. 8) (142 cm^3 cm^{-3}), CoMOF-74 (ref. 8) (136 cm^3 cm^{-3}), NOTT-100 (ref. 24) (139 cm^3 cm^{-3}), and higher than NOTT-119 (ref. 51) (134 cm^3 cm^{-3}), MOF-210 (ref. 1) (131 cm^3 cm^{-3}), DUT-4 (ref. 52) (124 cm^3 cm^{-3}), ZJU-32 (ref. 53) (120 cm^3 cm^{-3}), MOF-200 (ref. 1) (106 cm^3 cm^{-3}), indicating NJFU-3a as a potential material for CH_4 storage.

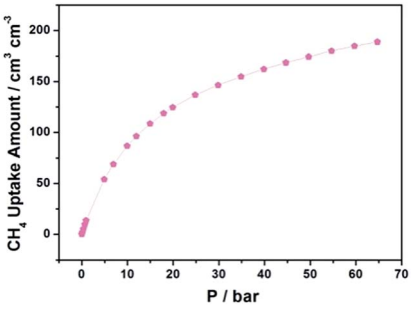

Fig. 4 Volumetric methane uptakes of NJFU-3a at 298 K in high pressure range.

Conclusions

In summary, we have developed a new organic linker of the V-shaped tetracarboxylic ligand with methoxyl group, and investigated the gases adsorption of the three-dimensional *mfj*-type metal–organic framework. The activated NJFU-3a exhibits moderate high porosity with the BET surface area of 2531.1 m^2 g^{-1}. Due to the unsaturated metal sites, suitable pore aperture and moderate high permanent porosity, NJFU-3a exhibits a high H_2 adsorption of 2.56 wt% at 77 K and 1 bar and a high CO_2 uptake of 15.8 wt% at 298 K and 1 bar. Meanwhile, a moderately high CH_4 storage of 155 cm^3 cm^{-3} at 35 bar and 298 K and a comparably high delivery amount of 135 cm^3 cm^{-3} was also observed in NJFU-3a when taking 5 bar as a specific lower pressure limit and 65 bar as the upper limit.

Acknowledgements

This work was supported by the Natural Science Fund of Jiangsu Province (Grant No. BK20140968 and BK20150798), the National Natural Science Foundation of China (Grant No. 21501094 and 21601047) and the priority academic program development of Jiangsu higher education institutions.

Notes and references

1 H. Furukawa, N. Ko, Y. B. Go, N. Aratani, S. B. Choi, E. Choi, A. O. Yazaydin, R. Q. Snurr, M. O'Keeffe, J. Kim and O. M. Yaghi, *Science*, 2010, **329**, 424–428.
2 S. Bureekaew, S. Horike, M. Higuchi, M. Mizuno, T. Kawamura, D. Tanaka, N. Yanai and S. Kitagawa, *Nat. Mater.*, 2009, **8**, 831–836.
3 S. Horike, K. Kishida, Y. Watanabe, Y. Inubushi, D. Umeyama, M. Sugimoto, T. Fukushima, M. Inukai and S. Kitagawa, *J. Am. Chem. Soc.*, 2012, **134**, 9852–9855.
4 V. Guillerm, D. Kim, J. F. Eubank, R. Luebke, X. Liu, K. Adil, M. S. Lah and M. Eddaoudi, *Chem. Soc. Rev.*, 2014, **43**, 6141–6172.
5 S. Yang, X. Lin, W. Lewis, M. Suyetin, E. Bichoutskaia, J. E. Parker, C. C. Tang, D. R. Allan, P. J. Rizkallah, P. Hubberstey, N. R. Champness, K. M. Thomas, A. J. Blake and M. Schroder, *Nat. Mater.*, 2012, **11**, 710–716.
6 C. E. Wilmer, O. K. Farha, T. Yildirim, I. Eryazici, V. Krungleviciute, A. A. Sarjeant, R. Q. Snurr and J. T. Hupp, *Energy Environ. Sci.*, 2013, **6**, 1158.
7 Y. Peng, V. Krungleviciute, I. Eryazici, J. T. Hupp, O. K. Farha and T. Yildirim, *J. Am. Chem. Soc.*, 2013, **135**, 11887–11894.
8 J. A. Mason, M. Veenstra and J. R. Long, *Chem. Sci.*, 2014, **5**, 32–51.
9 O. Shekhah, Y. Belmabkhout, Z. Chen, V. Guillerm, A. Cairns, K. Adil and M. Eddaoudi, *Nat. Commun.*, 2014, **5**, 4228.
10 Y. He, W. Zhou, G. Qian and B. Chen, *Chem. Soc. Rev.*, 2014, **43**, 5657–5678.

11 S. Ma and H. C. Zhou, *Chem. Commun.*, 2010, **46**, 44–53.
12 J. R. Li, J. Yu, W. Lu, L. B. Sun, J. Sculley, P. B. Balbuena and H. C. Zhou, *Nat. Commun.*, 2013, **4**, 1538.
13 X.-L. Qi, R.-B. Lin, Q. Chen, J.-B. Lin, J.-P. Zhang and X.-M. Chen, *Chem. Sci.*, 2011, **2**, 2214.
14 Z. Zhang, Y. Zhao, Q. Gong, Z. Li and J. Li, *Chem. Commun.*, 2013, **49**, 653–661.
15 Z. Lu, J. Bai, C. Hang, F. Meng, W. Liu, Y. Pan and X. You, *Chem.–Eur. J.*, 2016, **22**, 6277–6285.
16 L. Du, Z. Lu, K. Zheng, J. Wang, X. Zheng, Y. Pan, X. You and J. Bai, *J. Am. Chem. Soc.*, 2013, **135**, 562–565.
17 D. Sun, S. Ma, J. M. Simmons, J. R. Li, D. Yuan and H. C. Zhou, *Chem. Commun.*, 2010, **46**, 1329–1331.
18 D. Zhao, D. Yuan, A. Yakovenko and H. C. Zhou, *Chem. Commun.*, 2010, **46**, 4196–4198.
19 S. Yang, X. Lin, A. J. Blake, G. S. Walker, P. Hubberstey, N. R. Champness and M. Schroder, *Nat. Chem.*, 2009, **1**, 487–493.
20 B. Chen, N. W. Ockwig, A. R. Millward, D. S. Contreras and O. M. Yaghi, *Angew. Chem., Int. Ed.*, 2005, **44**, 4745–4749.
21 X. Lin, J. Jia, X. Zhao, K. M. Thomas, A. J. Blake, G. S. Walker, N. R. Champness, P. Hubberstey and M. Schroder, *Angew. Chem., Int. Ed.*, 2006, **45**, 7358–7364.
22 X. Lin, I. Telepeni, A. J. Blake, A. Dailly, C. M. Brown, J. M. Simmons, M. Zoppi, G. S. Walker, K. M. Thomas, T. J. Mays, P. Hubberstey, N. R. Champness and M. Schroder, *J. Am. Chem. Soc.*, 2009, **131**, 2159–2171.
23 S. Ma, D. Sun, J. M. Simmons, C. D. Collier, D. Yuan and H. C. Zhou, *J. Am. Chem. Soc.*, 2008, **130**, 1012–1016.
24 Y. He, W. Zhou, T. Yildirim and B. Chen, *Energy Environ. Sci.*, 2013, **6**, 2735.
25 X.-S. Wang, S. Ma, K. Rauch, J. M. Simmons, D. Yuan, X. Wang, T. Yildirim, W. C. Cole, J. J. López, A. d. Meijere and H.-C. Zhou, *Chem. Mater.*, 2008, **20**, 3145–3152.
26 S. Yang, X. Lin, A. Dailly, A. J. Blake, P. Hubberstey, N. R. Champness and M. Schroder, *Chem.–Eur. J.*, 2009, **15**, 4829–4835.
27 A. J. Cairns, J. A. Perman, L. Wojtas, V. Kravtsov, M. H. Alkordi, M. Eddaoudi and M. J. Zaworotko, *J. Am. Chem. Soc.*, 2008, **130**, 1560–1561.
28 X. S. Wang, S. Ma, P. M. Forster, D. Yuan, J. Eckert, J. J. Lopez, B. J. Murphy, J. B. Parise and H. C. Zhou, *Angew. Chem., Int. Ed.*, 2008, **47**, 7263–7266.
29 X. Liu, M. Park, S. Hong, M. Oh, J. W. Yoon, J. S. Chang and M. S. Lah, *Inorg. Chem.*, 2009, **48**, 11507–11509.
30 W. Qiu, J. A. Perman, L. Wojtas, M. Eddaoudi and M. J. Zaworotko, *Chem. Commun.*, 2010, **46**, 8734–8736.
31 C. Li, W. Qiu, W. Shi, H. Song, G. Bai, H. He, J. Li and M. J. Zaworotko, *CrystEngComm*, 2012, **14**, 1929.
32 J. J. t. Perry, V. Kravtsov, G. J. McManus and M. J. Zaworotko, *J. Am. Chem. Soc.*, 2007, **129**, 10076–10077.
33 D. Wang, B. Liu, S. Yao, T. Wang, G. Li, Q. Huo and Y. Liu, *Chem. Commun.*, 2015, **51**, 15287–15289.
34 Y. Liu, J. R. Li, W. M. Verdegaal, T. F. Liu and H. C. Zhou, *Chem.–Eur. J.*, 2013, **19**, 5637–5643.
35 Z. Lu, L. Du, K. Tang and J. Bai, *Cryst. Growth Des.*, 2013, **13**, 2252–2255.
36 K. Sumida, D. L. Rogow, J. A. Mason, T. M. McDonald, E. D. Bloch, Z. R. Herm, T. H. Bae and J. R. Long, *Chem. Rev.*, 2012, **112**, 724–781.
37 X. Duan, Y. Cui, Y. Yang and G. Qian, *CrystEngComm*, 2017, **19**, 1464–1469.
38 H.-M. Wen, G. Chang, B. Li, R.-B. Lin, T.-L. Hu, W. Zhou and B. Chen, *Cryst. Growth Des.*, 2017, **17**, 2172–2177.
39 S. Biswas, D. E. P. Vanpoucke, T. Verstraelen, M. Vandichel, S. Couck, K. Leus, Y.-Y. Liu, M. Waroquier, V. Van Speybroeck, J. F. M. Denayer and P. Van Der Voort, *J. Phys. Chem. C*, 2013, **117**, 22784–22796.
40 A. Demessence, D. M. D'Alessandro, M. L. Foo and J. R. Long, *J. Am. Chem. Soc.*, 2009, **131**, 8784–8786.
41 A. R. Millward and O. M. Yaghi, *J. Am. Chem. Soc.*, 2005, **127**, 17998–17999.
42 J. An, S. J. Geib and N. L. Rosi, *J. Am. Chem. Soc.*, 2009, **131**, 8376–8377.
43 T. K. Kim and M. P. Suh, *Chem. Commun.*, 2011, **47**, 4258–4260.
44 D. Yuan, D. Zhao, D. Sun and H. C. Zhou, *Angew. Chem., Int. Ed.*, 2010, **49**, 5357–5361.
45 S. Surble, F. Millange, C. Serre, T. Duren, M. Latroche, S. Bourrelly, P. L. Llewellyn and G. Ferey, *J. Am. Chem. Soc.*, 2006, **128**, 14889–14896.
46 J. B. Lin, W. Xue, J. P. Zhang and X. M. Chen, *Chem. Commun.*, 2011, **47**, 926–928.
47 O. K. Farha, A. O. Yazaydin, I. Eryazici, C. D. Malliakas, B. G. Hauser, M. G. Kanatzidis, S. T. Nguyen, R. Q. Snurr and J. T. Hupp, *Nat. Chem.*, 2010, **2**, 944–948.
48 W. Lu, D. Yuan, T. A. Makal, J. R. Li and H. C. Zhou, *Angew. Chem., Int. Ed.*, 2012, **51**, 1580–1584.
49 G. Q. Kong, Z. D. Han, Y. He, S. Ou, W. Zhou, T. Yildirim, R. Krishna, C. Zou, B. Chen and C. D. Wu, *Chem.–Eur. J.*, 2013, **19**, 14886–14894.
50 A. D. Wiersum, J.-S. Chang, C. Serre and P. L. Llewellyn, *Langmuir*, 2013, **29**, 3301–3309.
51 Y. Yan, S. Yang, A. J. Blake, W. Lewis, E. Poirier, S. A. Barnett, N. R. Champness and M. Schroder, *Chem. Commun.*, 2011, **47**, 9995–9997.
52 I. Senkovska, F. Hoffmann, M. Fröba, J. Getzschmann, W. Böhlmann and S. Kaskel, *Microporous Mesoporous Mater.*, 2009, **122**, 93–98.
53 J. Cai, X. Rao, Y. He, J. Yu, C. Wu, W. Zhou, T. Yildirim, B. Chen and G. Qian, *Chem. Commun.*, 2014, **50**, 1552–1554.

